Appl Nanosci (2016) 6:425–435
DOI 10.1007/s13204-015-0456-0

ORIGINAL ARTICLE

Magnetically retrievable nickel hydroxide functionalised AFe_2O_4 (A = Mn, Ni) spinel nanocatalyst for alcohol oxidation

Pooja B. Bhat[1] · **Badekai Ramachandra Bhat**[1]

Received: 11 March 2015 / Accepted: 29 April 2015 / Published online: 10 May 2015

Abstract Ultrasmall nickel hydroxide functionalised AFe_2O_4 (A = Mn, Ni) nanocatalyst was synthesized by traditional co-precipitation method and was examined for oxidation of aromatic alcohols to carbonyls using hydrogen peroxide as terminal oxidant. A very high surface area of 104.55 $m^2\ g^{-1}$ was achieved for ferromagnetic $MnFe_2O_4$ and 100.50 $m^2\ g^{-1}$ for superparamagnetic $NiFe_2O_4$, respectively. Efficient oxidation was observed due to the synergized effect of nickel hydroxide (bronsted base) on Lewis center (Fe) of the nanocatalyst. Catalyst recycling experiments revealed that the ultrasmall nanocatalyst can be easily recovered by external magnet and applied for nearly complete oxidation of alcohols for at least five successive cycles. Furthermore, the nickel hydroxide functionalised ultrasmall nanocatalyst exhibited higher efficiency for benzyl alcohol oxidation compared to $Ni(OH)_2$, bare $MnFe_2O_4$ and $NiFe_2O_4$. Higher conversion rate was observed for nickel hydroxide functionalised $NiFe_2O_4$ compared to $MnFe_2O_4$. Ultrasmall magnetic nickel hydroxide functionalised nanocatalyst showed environmental friendly, greener route for the oxidation of alcohols without significant loss in activity and selectivity within successive runs.

Keywords Nickel ferrite · Manganese ferrite · Nanoparticles · Oxidation

✉ Badekai Ramachandra Bhat
ram@nitk.edu.in

[1] Catalysis and Materials Chemistry Laboratory, Department of Chemistry, National Institute of Technology Karnataka, Srinivasanagar, Surathkal 575025, India

Introduction

Extensive research has been devoted in recent years to develop environmental friendly metal catalysts for various oxidation reactions. Noble metals such as gold (Ma et al. 2009; Costa et al. 2012), palladium (Laska et al. 2009) and ruthenium (Jacinto et al. 2009) have been employed and have been demonstrated as good oxidizing catalyst. However, their high cost, less sensitivity at higher temperatures and scarcity make noble metal catalysts less desirable. Hence, to develop cost effective, noble metal free and good performance catalysts have been considered as a prime importance by researchers. Spinel ferrites are promising candidates since they are less expensive, earth abundant and environmental friendly (Jacobs et al. 1994; Ramankutty and Sugunan 2001). Ferrite catalysts have found to be less active to catalyze alcohol oxidation reactions under mild conditions (Shi et al. 2007). But few researchers have achieved higher catalytic activity by increasing surface area and modification of ferrite structure with cations (Khan and Smirniotis 2008).

In this paper, we report the synthesis of nickel hydroxide functionalised superparamagnetic nickel ferrite and ferromagnetic manganese ferrite nanocatalyst. It was evaluated for its catalytic activity in alcohol oxidation reactions. To the best of our knowledge, nickel hydroxide functionalised AFe_2O_4 (A = Mn, Ni) nanocatalyst has not been reported as the catalyst for the oxidation of alcohols using mild oxidizing agent. Nickel hydroxide was chosen as a cation due to the possibility of higher synergetic effect. This resulted in higher catalytic activity. XRD and FTIR results confirm the surface modification of ferrite particles by nickel hydroxide. The size of nanocatalyst was found to be around 10–20 nm for nickel hydroxide functionalized $MnFe_2O_4$ and 20–60 nm for nickel hydroxide functionalized $NiFe_2O_4$. Surface area of

104.55 and 100.50 $m^2\ g^{-1}$ was achieved for nickel hydroxide functionalized $MnFe_2O_4$ and $NiFe_2O_4$, respectively. The synthesized nickel ferrite nanocatalyst exhibited superparamagnetism at room temperature. Ferromagnetic property was observed for manganese ferrite nanocatalyst. The nickel hydroxide functionalised ferrite nanocatalyst showed better catalytic activity towards the oxidation of alcohols by mild oxidizing agent due to higher synergistic effect. The green synthetic route, magnetically recoverable and higher catalytic activity of synthesized nano nickel hydroxide functionalized ferrite catalyst would be a promising solution for the oxidation of alcohols to corresponding carbonyls using mild oxidizing agents.

Experimental

Materials

Ferrous chloride, ferric chloride, manganese chloride and nickel chloride were purchased from Merck, India and used as received. 3-Aminopropyltriethoxysilane was purchased from Sigma-Aldrich and used without further purification.

Synthesis of magnetic ferrite

Magnetic $MnFe_2O_4$ and $NiFe_2O_4$ were prepared by co-precipitation technique. The method involved slow addition of 25 % ammonia solution to the salts of manganese and nickel with ferric chloride (1:2) under anaerobic condition at 80 °C. The black precipitate obtained was aged overnight, washed with ethanol, water and dried at 80 °C.

Synthesis of surface functionalized magnetic ferrite

Synthesized and purified $MnFe_2O_4$ and $NiFe_2O_4$ nanoparticles (1 g) were modified using 3-aminopropyltriethoxysilane (APTES, 0.5 g) in the presence of toluene at 80 °C for 6 h in argon atmosphere. The product was aged for 1 h and centrifuged with toluene, ethanol and dried at 80 °C. The obtained aminosilane modified ferrite (2 g) was vigorously stirred with aqueous solution of $NiCl_2.7H_2O$ (0.6 g) at room temperature for 24 h at pH 13 by the addition of an aqueous solution of NaOH (1 N). The obtained nickel hydroxide functionalized $MnFe_2O_4$, $NiFe_2O_4$ was washed with deionized water, ethanol and dried at 80 °C. The functionalized product was then characterized by different techniques such as XRD, SEM and TEM.

Oxidation reactions

All reactions were carried out in a glass reactor ($\sim$50 mL). Benzyl alcohol (1 mmol), nano functionalized nickel ferrite catalyst (0.04 g), manganese ferrite catalyst (0.04 g) and acetonitrile (3 mL) were added and mixed in respective glass reactor. H_2O_2 (30 wt% in water, 10.0 mmol) was added as a mild oxidant and the reaction mixture was vigorously stirred at 80 °C for 7 h. The aliquots of the mixture after reaction were analyzed by GC. The retention time for different compounds was determined by injecting pure compounds under identical GC conditions.

Characterization

Powder X-ray diffraction (XRD) measurement was performed on JEOL JDX 8P diffractometer. The diffraction patterns were recorded at room temperature with Cu Kα radiation ($\lambda = 1.5418$ Å) at a scan rate of 2 °/min to determine the crystallinity of the sample. The FTIR spectra were measured on JASCO FTIR-4200 (KBr technique). The UV–Vis spectra were recorded in analytikjena SPECORD S600. Surface morphology and composition were studied by field emission gun scanning electron microscopy (FESEM) JSM-7600F and transmission electron microscope (TEM) Philips CM200. Surface area and pore size distribution were studied by Gemini V2.00 surface analyzer. The magnetic properties were determined by Lakeshore VSM 7410 Vibrating Sample Magnetometer at room temperature. The reaction product analysis was carried out using Gas Chromatography (GC) (Shimadzu 2014, Japan), siloxane Restek capillary column (30 m length and 0.25 mm diameter) and Flame Ionization Detector. The column temperature was increased at the rate of 10 °C/min. Nitrogen gas was used as the carrier gas.

Results and discussion

Characterization of the catalyst

Structure and crystallinity of nickel hydroxide functionalised AFe_2O_4 (A = Mn, Ni) nanocatalyst were analyzed by X-ray diffraction method. Figure 1 shows the XRD diffraction pattern of the ferrite nanocatalyst and nickel hydroxide functionalised AFe_2O_4 (A = Mn, Ni) nanocatalyst. The characteristic peaks observed at $2\theta = 30.0°$, 35.40°, 43.2°, 53.6°, 57.2°, 62.0° correspond to (220), (311), (400), (422), (511) and (440) diffraction phases of bare Fe_3O_4 (JCPDS no. 19-0629). The presence of new diffraction peaks observed at 33.0°, 38.8° and 59.6° can be indexed with (100), (101) and (110) diffraction planes of nickel hydroxide, respectively (JCPDS 14-0117). Nickel hydroxide is chemisorbed on the ultrasmall nanocatalyst. The lone pairs present on nitrogen of aminosilane coordinates with $Ni(OH)_2$ to form a catalyst. The diffractogram exhibits sharp lines indicating that the nanocatalyst sample

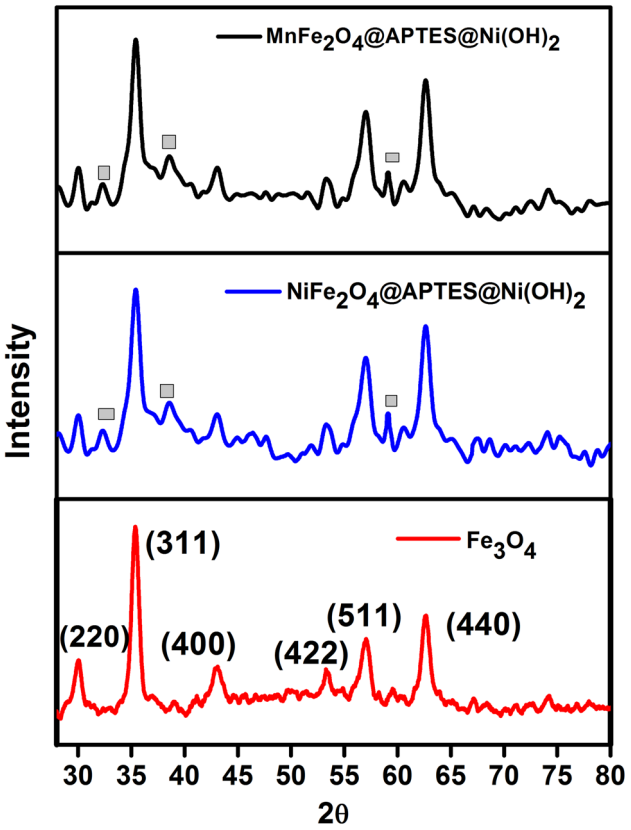

Fig. 1 X-ray diffractogram of the catalyst

is highly crystalline. The average crystallite size was calculated from XRD using Debye Scherer equation with the help of full width half maxima (FWHM) of the diffraction peaks (Eq. 1):

$$D = 0.9\lambda/B\cos\theta \quad (1)$$

where B is the FWHM of the diffraction peak at 2θ recorded using X-rays of wavelength $\lambda = 1.54$ Å. The average crystallite size was found to be 10 nm for $MnFe_2O_4$ and 40 nm for $NiFe_2O_4$,respectively. Energy dispersive X-ray analysis (EDX) was also performed to analyze the elements and EDX spectrum confirms the presence of 'Ni', 'Fe', 'Si', 'O' and 'Mn' elements in the nanocatalyst (Fig. 2).

The FTIR bands of the solids in the range of 100–1000 cm^{-1} are usually assigned to ions in the crystal lattice. The basic characteristic peak observed at 583 cm^{-1} corresponds to Fe–O vibration (Phan and Jones 2006). Broad bands of –OH stretch at 3351 cm^{-1} and deformation vibration at 1640 cm^{-1} were observed due to physisorbed water and surface hydroxyl groups. An additional peak at 1406 cm^{-1} was observed in functionalized nanocatalyst spectrum clearly confirming the aminosilane functionalization (Fig. 3). The functionalization of aminosilane on nanocatalyst was further confirmed by UV–visible analysis and UV–visible spectra exhibited absorbance at around 330 nm due to charge transfer further confirming Si–O adsorption on the ferrite catalyst (Fig. 4).

The morphology and size of synthesized nanocatalyst was studied using FEG-SEM and TEM techniques and images are shown in Figs. 5, 6. From FEG-SEM image, highly agglomerated small particles of size around 10–20 nm were observed for nickel hydroxide functionalized $MnFe_2O_4$ and 20–60 nm for nickel hydroxide functionalized $NiFe_2O_4$ (Figs. 5a, 6a). TEM image clearly signifies that nanocatalyst is composed of spherical nanoparticles. Range of particle sizes from 10–20 nm and 20–60 nm was achieved for nickel hydroxide functionalized $MnFe_2O_4$ and $NiFe_2O_4$, respectively. The observance of smoothened surface on nanocatalyst indicates the hydroxide dispersion of nickel hydroxide on nanocatalyst.

The surface area of synthesized nanocatalyst was also determined using BET surface area analyzer using adsorption data over the relative pressure ranging from 0.05 to 0.3. A high BET surface area of 104.55 $m^2\ g^{-1}$ for manganese ferrite and 100.50 $m^2\ g^{-1}$ for nickel ferrite was achieved compared to the earlier reports (Chen and He 2001; Lahiri and Sengupta 1991; Zhang et al. 2013). Figure 7a, b exhibits a typical type-IV isotherm indicating mesoporosity was observed (Singh 1985). The BJH pore size distribution (inset) showed a narrow pore size distribution of the catalyst due to smaller sized nanoparticles.

The room temperature magnetic property of synthesized nanocatalyst was also analyzed using Vibrating Sample Magnetometry and corresponding result curve is shown in Fig. 8. The data revealed that nanocatalyst exhibited superparamagnetism property for nickel ferrite at room temperature. The saturation magnetization observed was low for particle size in range of 20–60 nm due to non-collinear spin arrangement near the surface of the nanoparticle (Niasari et al. 2009). A linear M-H curve with a very small hysteresis loop exhibiting ferromagnetic nature was obtained for manganese ferrite. The very small spin magnetic moment in nanoparticles <20 nm cannot collate each other and hence forms a linear M-H curve (Lee and Hyeon 2012; Vamvakidis et al. 2013).

Catalytic oxidation of alcohols

Recently, many researchers have employed ferrite as catalyst for benzyl alcohol oxidation. Shi et al. (2008) observed a maximum of 33 % conversion with 95 % selectivity for benzyl alcohol oxidation with free nano iron oxide. Researchers have explored different ways to enhance catalytic activity for alcohol oxidation by impregnating ferrite with different supports (Polshettiwer and Varma 2009; Oliveira et al. 2010; Kotani et al. 2006; Zhang et al. 2008; Bhat et al. 2014; Bhat and Bhat 2015).

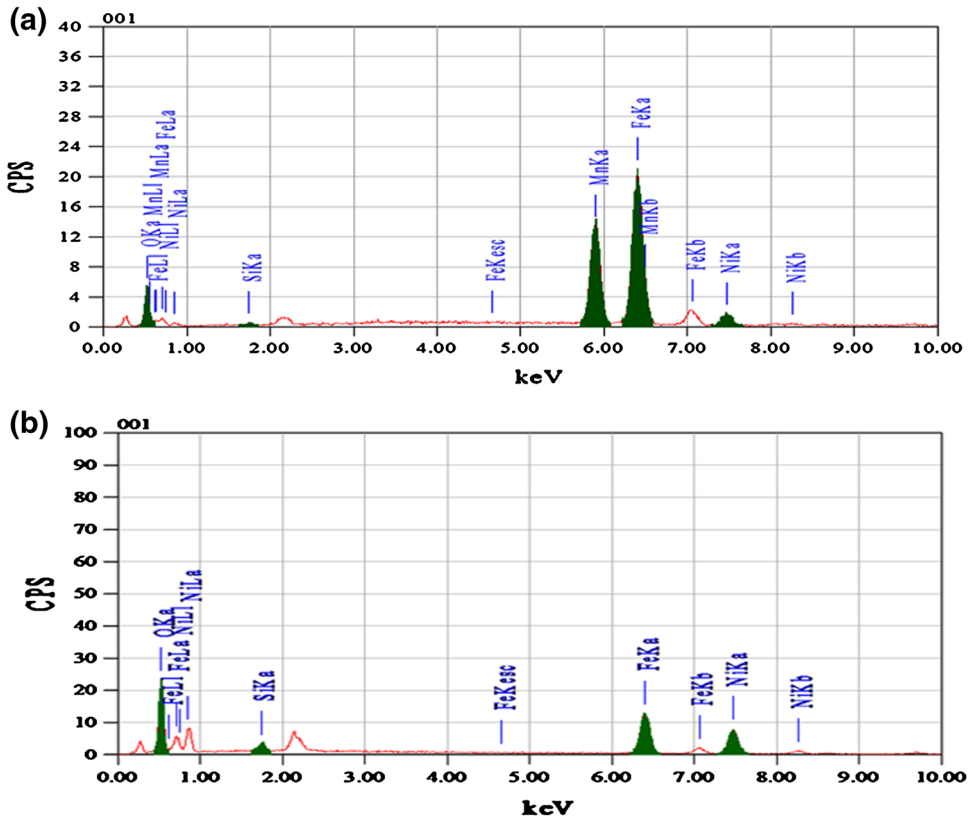

Fig. 2 Energy dispersive X-ray analysis of **a** $MnFe_2O_4$@APTES@$Ni(OH)_2$ and **b** $NiFe_2O_4$@APTES@$Ni(OH)_2$

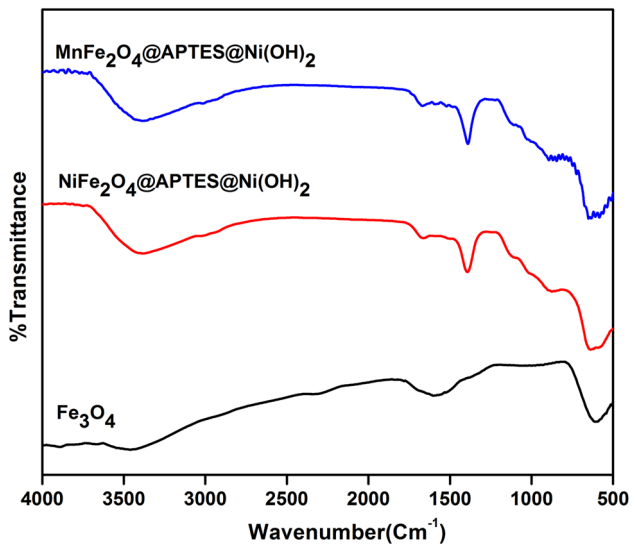

Fig. 3 FTIR spectra of the nanocatalyst

The synthesized nanocatalyst provides an alternative inexpensive catalyst for efficient oxidation of alcohols.

Oxidation of benzyl alcohol as a model substrate was initially investigated to optimize the reaction conditions such as the influence of solvent, temperature, alcohol/oxidant molar ratio and length of the reaction time (Table 1).

The effect of different bases such as KOH and pyridine on alcohol oxidation was studied (Fig. 9a, b) and base facilitated deprotonation of alcohol activity was observed. In this study, aminosilane catalyst was considered as model catalyst for oxidation of alcohols. The enhanced catalytic activity and the selectivity of the nanocatalyst with different bases [strong base; KOH, inorganic base; $Cs(CO)_3$, organic base; pyridine (lone nitrogen forms complex with catalyst)] as additives were studied. This was compared with catalytic activity of nanocatalyst without base and supported magnetic nanocatalyst. It is clear from these results that synergized effect of magnetic nanocatalyst provides more selective reaction for aldehyde than the other catalyst with additives.

The effect of concentration of catalyst in oxidation of alcohols with respect to model substrate showed significant conversion for 0.04 g of catalyst (Table 1, Entry 4). The conversion was less in the absence of the catalyst (Table 1, Entry 1) and signifies the catalytic role of ultrasmall nanoparticles. The conversion reduced with increase in amount of the nanocatalyst (Table 1, Entry 5). This may be due to decrease in surface area of the catalyst due to adsorption of oxidized products on the active sites. The conversion rate was less in absence of the oxidant (Table 1, entry 7). This confirmed that a minimum quantity of 10 mmol of H_2O_2 was necessary for effective oxidation of

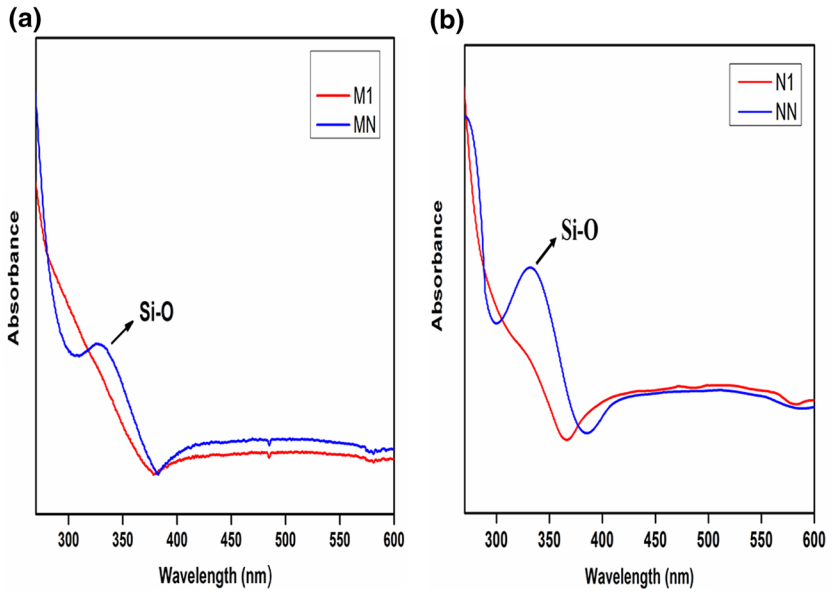

Fig. 4 UV–Visible spectra of **a** Manganese ferrite and **b** nickel ferrite

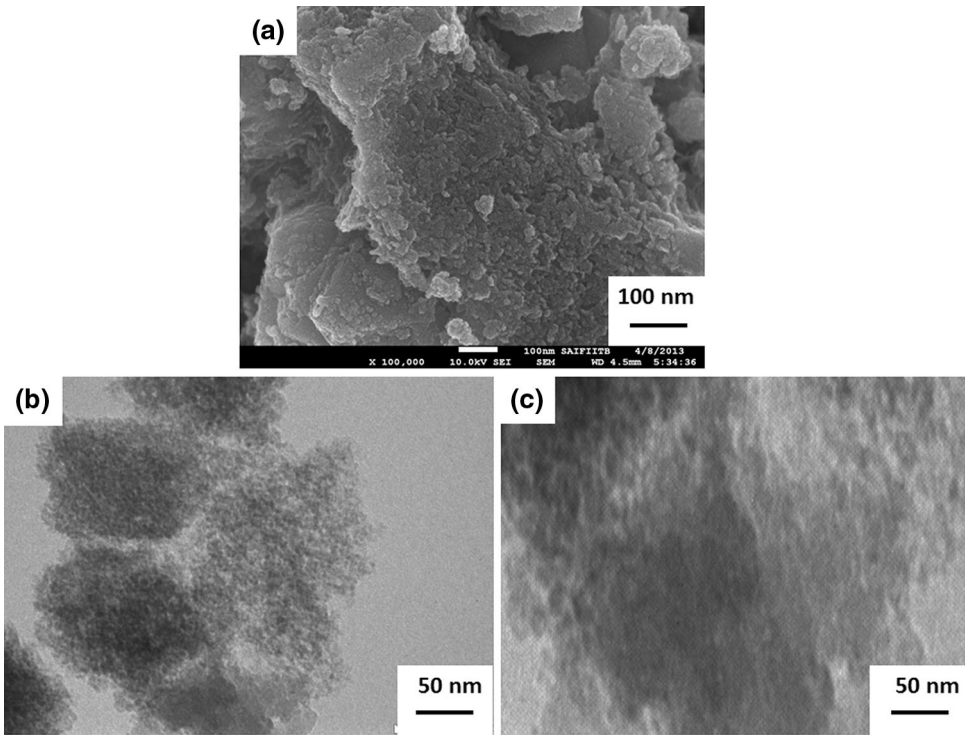

Fig. 5 **a** FESEM, **b** TEM and **c** dispersed $Ni(OH)_2$ images of $MnFe_2O_4$@APTES@$Ni(OH)_2$ catalyst

alcohols. The product analysis was done at regular intervals of time under similar reaction conditions to study the effect of time on the activity. It was observed that the GC yield remained constant after a reaction time of 7 h (Fig. 9c). It was observed that the conversion rate for $NiFe_2O_4$ was high compared to $MnFe_2O_4$. Agglomeration plays a crucial role in nanocatalysis. Superparamagnetic nanoparticles have fewer tendencies for agglomeration due to very small spin magnetic moment than ferromagnetic nanoparticles. It is also dependent on temperature, surface energy, smaller particle size and surface tension of liquids during the course of reaction. Small sized particles tend to form agglomerates to reduce the energy associated with the high surface area to volume ratio of the nanosized particles. However, when the size of the nanoparticle is reduced too small 10–20 nm, then each particle becomes single magnetic domain and shows superparamagnetism. Interparticle attractions in superparamagnetic nanoparticles are dependent on variation in temperature. At room temperature, agglomeration is negligible in superparamagnetic materials

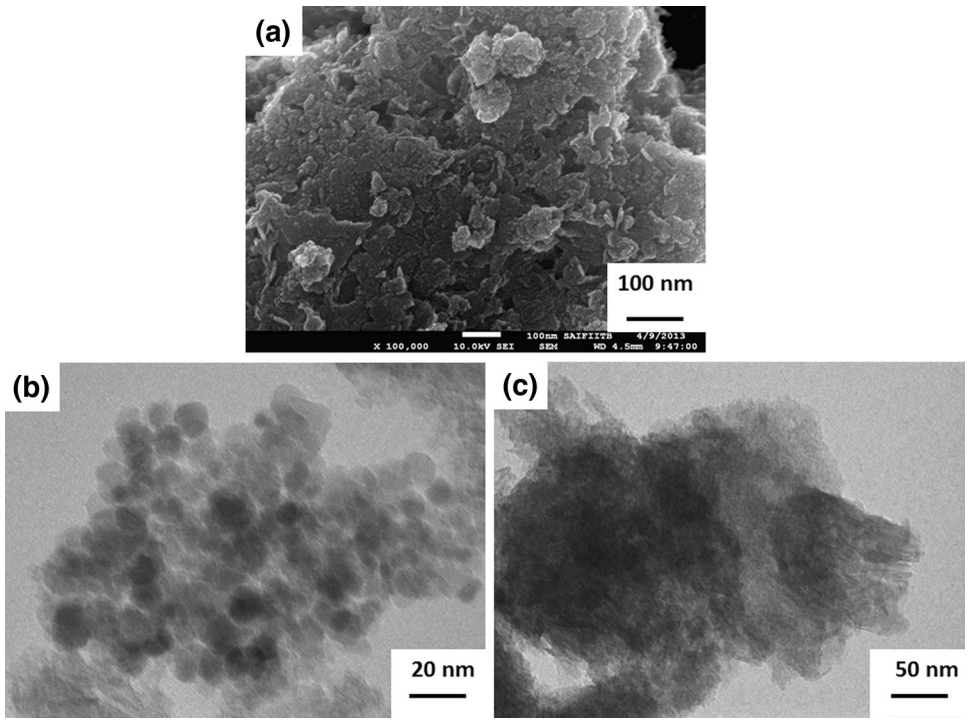

Fig. 6 **a** FESEM, **b** TEM and **c** dispersed $Ni(OH)_2$ images of $MnFe_2O_4$@APTES@$Ni(OH)_2$ catalyst

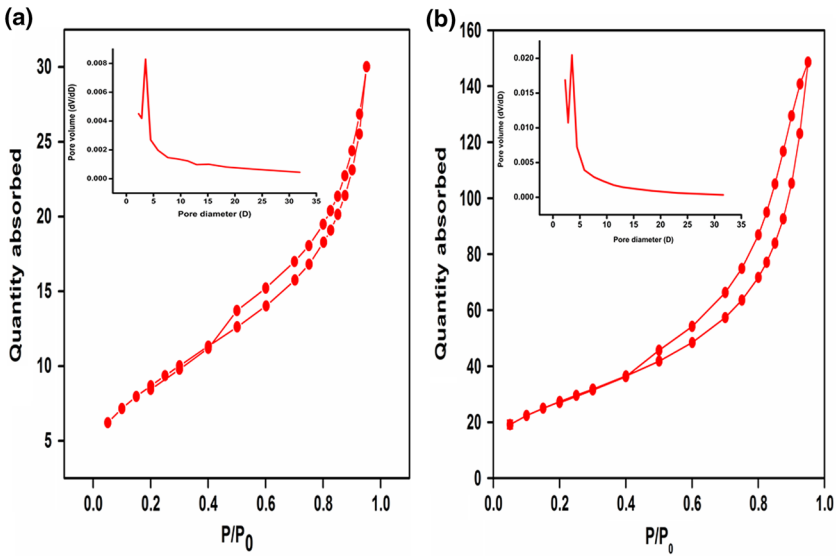

Fig. 7 Nitrogen sorption isotherm and pore size distribution of **a** $MnFe_2O_4$@APTES@$Ni(OH)_2$ and **b** $NiFe_2O_4$@APTES@$Ni(OH)_2$ nanocatalyst

as they act as an individual single domain particle with high magnetic response. However, with increase in temperature, enhancement of interparticle attractions is usually observed which can lead to agglomerates. Thus, the small sized ferromagnetic nanoparticles are prone to reduce the accessible reactive centers due to agglomeration. Hence, higher conversion rate was observed for nickel hydroxide functionalised $NiFe_2O_4$.

The observed conversion rate for $MnFe_2O_4$@APTES@$Ni(OH)_2$ and $NiFe_2O_4$@APTES@$Ni(OH)_2$ nanocatalyst for the same optimized reaction condition was high compared to bare manganese ferrite (48.3 %), nickel ferrite (52.4 %) and $Ni(OH)_2$ (15.2 %) alone. This further confirmed the synergised effect of bronsted base $Ni(OH)_2$ on ferrite.

Further, the oxidation was extended to a variety of aromatic and aliphatic alcohols using the optimized reaction conditions. The oxidation results for the variety of alcohols are summarized in Table 2. Aromatic substituent was found to be more reactive than aliphatic alcohols which can be attributed due to its delocalization. Similarly, electron donating groups were found to slow down

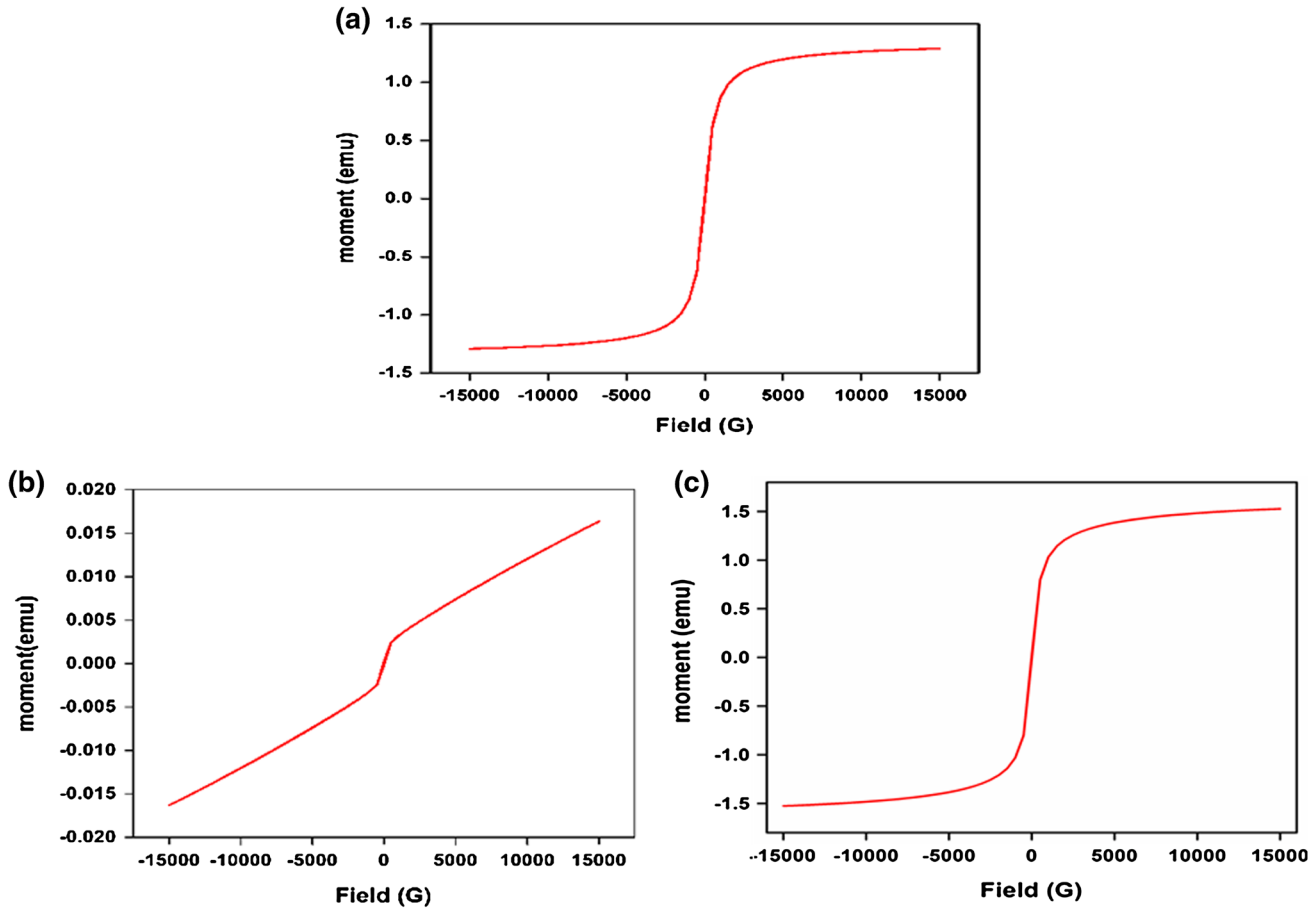

Fig. 8 M-H curve of **a** Fe_3O_4 **b** $MnFe_2O_4$@APTES@$Ni(OH)_2$ and **c** $NiFe_2O_4$@APTES@$Ni(OH)_2$ nanocatalyst

Table 1 Optimization of reaction conditions for oxidizing benzyl alcohol to benzaldehyde

Entry	Catalyst (g)	Amount of oxidant (mmole)	Conversion (%)[a]	
			MN	NN
1	**0**	**10.0**	**0.6**	**1.8**
2	0.01	10.0	34.7	55.3
3	0.02	10.0	58.4	65.4
4	**0.04**	**10.0**	**78.7**	**82.4**
5	0.06	10.0	64.5	57.3
6	0.08	10.0	43.2	40.0
7	**0.04**	**0**	**1.4**	**3.34**
8	0.04	5.0	16.2	18.6

[a] Reaction conditions: 1 mmol substrate; 10 mmol oxidant (30 wt% H_2O_2), 3 mL acetonitrile, time (7 h). Conversion determined by GC

oxidation whereas electron withdrawing groups accelerated the reaction. Among the various alcohols studied phenylethanol showed maximum conversion with a GC yield of 96.0 %. The catalyst was easily recovered by external magnet after the reaction and can be reused without the significant loss of the catalytic activity and selectivity. Reusability study confirmed that the catalyst could be used effectively for alcohol oxidation for at least 5 cycles (Fig. 10).

Magnetic nanoparticles have a large constant magnetic moment and behave like a giant paramagnetic atom with a fast response to applied magnetic field. Hence, during the course of reaction, the catalyst can be extracted by simple attraction to external magnet. This avoids conventional laborious purification of the catalyst by filtration or extraction and thus renders greenness to the catalyst.

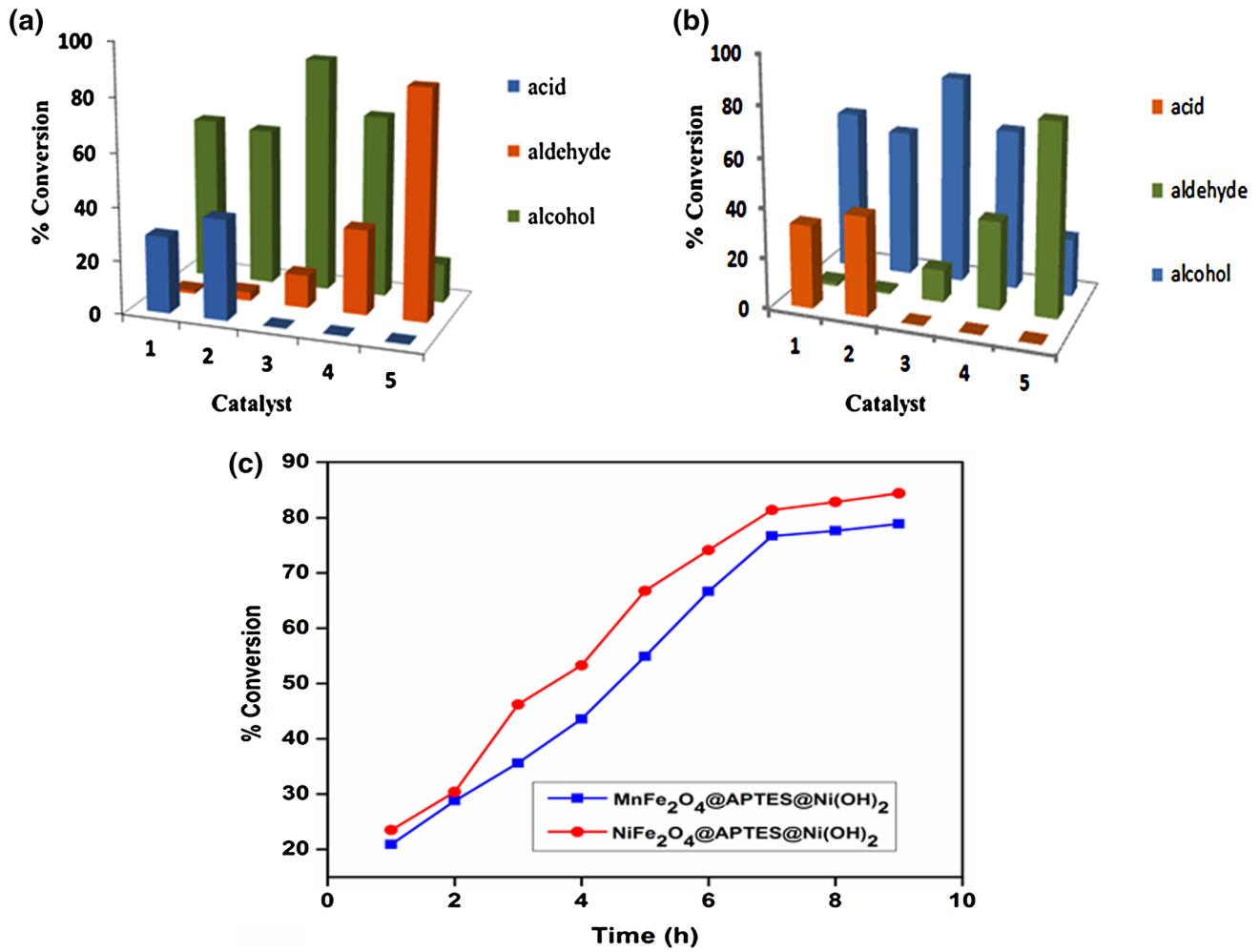

Fig. 9 Effect of base as additives on aminosilane modified **a** $MnFe_2O_4$ and **b** $NiFe_2O_4$; *1* KOH (0.25 mmol), *2* pyridine (0.25 mmol), *3* $Cs(CO_3)_2$ (0.25 mmol), *4* without base and *5* $Ni(OH)_2$ enveloped catalyst. **c** Effect of time on the catalyst

Conclusions

In conclusion, the synthesized magnetic nanocatalyst exhibited higher catalytic activity and selectivity for the oxidation of alcohols due to synergistic effect of nickel hydroxide (bronsted base) on the nanocatalyst. An ultrasmall nickel hydroxide functionalized ferromagnetic $MnFe_2O_4$ and a superparamagnetic $NiFe_2O_4$ nanoparticle were successfully synthesized by chemical co-precipitation method. The size of synthesized nanocatalyst was in the range of 10–20 nm with surface area of 104.55 $m^2\ g^{-1}$ for $MnFe_2O_4$@APTES@$Ni(OH)_2$ and 20–60 nm with surface area of 100.55 $m^2\ g^{-1}$ for $NiFe_2O_4$@APTES@$Ni(OH)_2$. This study offers a promising ultrasmall magnetically recoverable nanocatalyst for oxidation of aromatic alcohols to corresponding carbonyls with high conversion factor by greener route.

Table 2 Catalytic activity of $MnFe_2O_4$@ APTES@ $Ni(OH)_2$ (MN) and $NiFe_2O_4$@ APTES@ $Ni(OH)_2$ (NN) for alcohol oxidation

Entry	Substrate	Conversion (%)*		Product
		MN	NN	
1	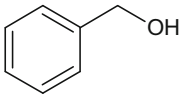	78.7	82.4	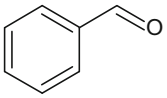
2	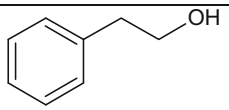	96.3	97.6	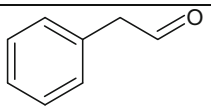
3	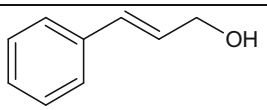	94.3	95.3	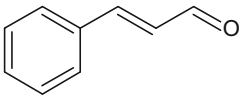
4	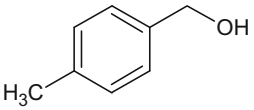	65.5	66.6	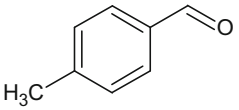
5	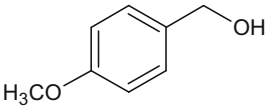	61.2	62.5	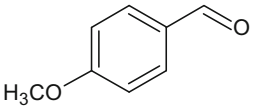
6	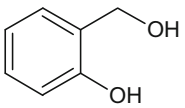	59.6	60.4	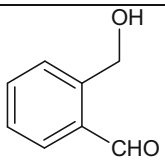
7	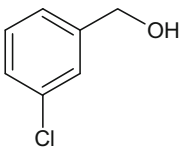	69.8	76.6	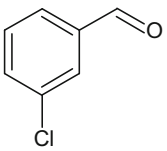
8	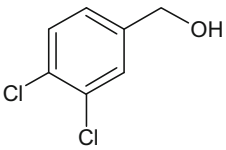	73.5	74.4	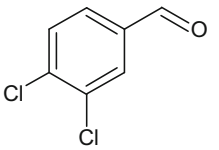
9	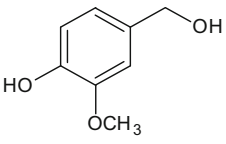	65.5	66.9	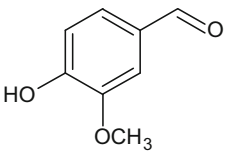
10	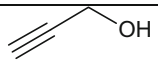	38.3	43.7	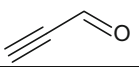
11	$(CH_3)_2CH_2OH$	29.6	31.4	$(CH_3)_2CH_2CHO$

[a] Substrate (1.0 mmol); 0.04 g catalyst; acetonitrile (3.0 mL), oxidant (10 mmol), time (7 h). Conversion and selectivity were determined by GC. Average of GC 3 trials

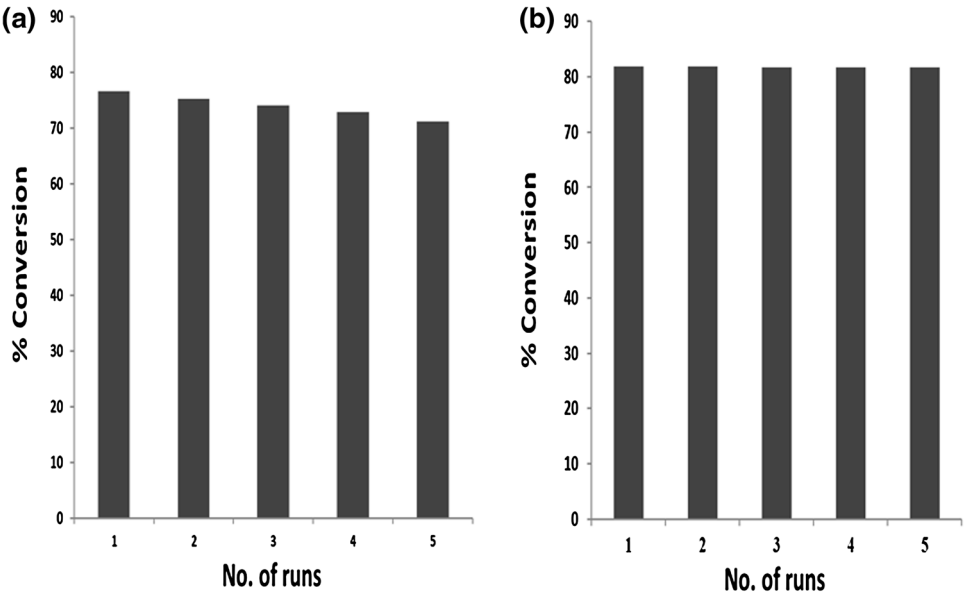

Fig. 10 Recyclability of **a** $MnFe_2O_4$@APTES@$Ni(OH)_2$ and **b** $NiFe_2O_4$@APTES@$Ni(OH)_2$ nanocatalyst

Acknowledgments The author Miss Pooja thanks NITK, Surathkal for research fellowship, Dr. Ravindra for good inputs, IIT Bombay (CRNTS) for FESEM and TEM analysis. We also thank NIT Trichy for BET surface area analysis.

References

Bhat PB, Bhat BR (2015) Nano Fe_3O_4@APTES@$Ni(OH)_2$ as a catalyst for alcohol oxidation. New J Chem 39:273–278

Bhat PB, Inam F, Bhat BR (2014) Nickel hydroxide/cobalt–ferrite magnetic nanocatalyst for alcohol oxidation. ACS Combin Sci 16(8):397–402

Chen DH, He XR (2001) Synthesis of nickel ferrite nanoparticles by sol-gel method. Mater Res Bull. 36:1369–1377

Costa VV, Estrada M, Demidova Y, Prosvirin I, Kriventsov V, Cotta RF, Fuentes S, Simakov A, Gusevskaya EV (2012) Gold nanoparticles supported on magnesium oxide as catalysts for the aerobic oxidation of alcohols under alkali-free conditions. J Catal 292:148–156

Jacinto MJ, Santos OHCF, Jardim RF, Landers R, Rossi LM (2009) Preparation of recoverable Ru catalysts for liquid-phase oxidation and hydrogenation reactions. Appl Catal A Gen 360:177–182

Jacobs JP, Maltha A, Reitjes JGH, Drimal J, Ponec V, Brongersma HH (1994) The surface of catalytically active spinels. J Catal 47:294–300

Khan A, Smirniotis PG (2008) Relationship between temperature-programmed reduction profile and activity of modified ferrite-based catalysts for WGS reaction. J Mol Catal A Chem 280:43–51

Kotani M, Koike T, Yamaguchi K, Mizuno N (2006) Ruthenium hydroxide on magnetite as a magnetically separable heterogeneous catalyst for liquid-phase oxidation and reduction. Green Chem 8:735–741

Lahiri P, Sengupta SK (1991) Spinel ferrites as catalysts: a study on catalytic effect of coprecipitated ferrites on hydrogen peroxide decomposition. Can J Chem 69:33–36

Laska U, Frost CG, Price GJ, Plucinski PK (2009) Easy-separable magnetic nanoparticle-supported Pd catalysts: kinetics, stability and catalyst re-use. J Catal 268:318–328

Lee N, Hyeon T (2012) Designed synthesis of uniformly sized iron oxide nanoparticles for efficient magnetic resonance imaging contrast agents. Chem Soc Rev 41:2575–2589

Ma CY, Dou BJ, Li JJ, Cheng J, Hu Q, Hao ZP, Qiao SZ (2009) Catalytic oxidation of benzyl alcohol on Au or Au–Pd nanoparticles confined in mesoporous silica. Appl Catal B Environ. 92:202–208

Niasari MS, Davar F, Mahmoudi T (2009) A simple route to synthesize nanocrystalline nickel ferrite ($NiFe_2O_4$) in the presence of octanoic acid as a surfactant. Polyhedron 28:1455–1458

Oliveira RL, Kiyohara PK, Rossi LM (2010) High performance magnetic separation of gold nanoparticles for catalytic oxidation of alcohols. Green Chem 12:144–149

Phan NTS, Jones CW (2006) Highly accessible catalytic sites on recyclable organosilane-functionalized magnetic nanoparticles: an alternative to functionalized porous silica catalysts. J Mol Catal A Chem 253:123–131

Polshettiwer V, Varma RS (2009) Nanoparticle-supported and magnetically recoverable palladium (Pd) catalyst: a selective and sustainable oxidation protocol with high turnover number Org. Biomol Chem 7:37–40

Ramankutty CG, Sugunan S (2001) Surface properties and catalytic activity of ferrospinels of nickel, cobalt and copper, prepared by soft chemical methods. Appl Catal A Gen 218:39–51

Shi F, Tse MK, Pohl M, Brückner A, Zhang S, Beller M (2007) Tuning catalytic activity between homogeneous and heterogeneous catalysis: improved activity and selectivity of free nano-Fe2O3 in selective oxidations. Angew Chem Int Ed 47:8866–8868

Shi F, Tse MK, Pohl M, Radnik J, Brückner A, Zhang S, Beller M (2008) Nano-iron oxide-catalyzed selective oxidations of alcohols and olefins with hydrogen peroxide. J Mol Catal A Chem 292:28–35

Singh KSW (1985) Reporting physisorption data for gas/solid systems with Special Reference to the determination of surface area and porosity. Pure Appl Chem 57:603–619

Vamvakidis K, Sakellari D, Angelakeris M, Samara CD (2013) Size and compositionally controlled manganese ferrite nanoparticles with enhanced magnetization. J Nanopart Res 15:1743–1754

Zhang DH, Li GD, Li JX, Chen JS (2008) One-pot synthesis of Ag–Fe_3O_4 nanocomposite: a magnetically recyclable and efficient catalyst for epoxidation of styrene. Chem Commun 29:3414–3416

Zhang Z, Wang Y, Tan Q, Zhong Z, Su F (2013) Facile solvothermal synthesis of mesoporous manganese ferrite ($MnFe_2O_4$) microspheres as anode materials for lithium-ion batteries. J Colloid Interface Sci 398:185–192